Inorg. Chem. **2005**, *44*, 7503–7510

Role of Anions on the Crystal Structures of Copper(II) and Zinc(II) Complexes of a Tunable Butterfly Cyclophane Macrocycle

Martin Chadim,[†] Pilar Díaz,[‡] Enrique García-España,*[,‡] Jana Hodačová,*[,†] Julio Latorre,[§] Malva Liu-González,[||] Santiago V. Luis,[⊥] José M. Llinares,[‡] and Jiří Závada[†]

Institute of Organic Chemistry and Biochemistry, Academy of Sciences of the Czech Republic, Flemingovo nam. 2, 166 10 Prague 6, Czech Republic, Departamento de Química Inorgánica, Instituto de Ciencia Molecular, Universidad de Valencia, c/ Dr. Moliner 50, 46100 Burjassot, Valencia, Spain, Departamento de Química Inorgánica, Instituto de Materiales, Universidad de Valencia, c/ Dr. Moliner 50, 46100 Burjassot, Valencia, Spain, Departamento de Química Inorgánica y Orgánica, UAMOA, Universitat Jaume I/CSIC, 12080 Castellón, Spain, and SCSIE, Universidad de Valencia, c/ Dr. Moliner 50, 46100 Burjassot, Valencia, Spain

Received July 1, 2005

Three crystal structures of a ditopic cyclophane ligand (**L**) in which two 1,5,8,12-tetraamine molecules have been attached through methylene spacers to the ortho positions of a benzene ring are reported. The first one (**1**) corresponds to the tetraprotonated free macrocycle (H_4L^{4+}) having two tetrachlorozincate(II) counteranions ($C_{24}H_{54}O_2N_8Cl_8Zn_2$, $a = 9.1890(2)$ Å, $b = 14.0120(3)$ Å, $c = 15.3180(3)$ Å, $\alpha = 89.2320(7)°$, $\beta = 82.0740(6)°$, $\gamma = 83.017(1)°$, $Z = 2.00$, triclinic, $P\bar{1}$); the second one (**2**) is of a binuclear Cu^{2+} complex having coordinated chloride anions and perchlorate counteranions ($C_{24}H_{58}O_{14}N_8Cl_4Cu_2$ $a = 9.9380(2)$ Å, $b = 30.2470(6)$ Å, $c = 53.143(1)$ Å, orthorhombic, $F2dd$, $Z = 18$), and the third one (**3**) corresponds to an analogous Zn^{2+} complex that has been crystallized using triflate as counteranion ($C_{26}H_{51.2}O_{6.6}N_8Cl_2F_6S_2Zn_2$ $a = 8.472(5)$ Å, $b = 9.310(5)$, $c = 13.745(5)$ Å, $\alpha = 84.262(5)°$, $\beta = 77.490(5)°$, $\gamma = 73.557(5)°$, triclinic, $P\bar{1}$, $Z = 2$). The analysis of the crystallographic data clearly shows that the conformation of the macrocycle and, in consequence, the overall architecture of the crystals are controlled by the anions present in the moiety, π–π-stacking associations, and hydrogen bonding interactions. The protonation and stability constants for the formation of the Cu^{2+} and Zn^{2+} complexes in aqueous solution have been determined potentiometrically in 0.15 mol dm^{-3} $NaClO_4$ at 298.1 K. Intramolecular hydrogen bonding defines the protonation behavior of the compound. Positive cooperativity is observed in the formation of the Cu^{2+} complexes.

Introduction

Since the initial guesses in the 1960s looking for the way in which molecules establish their contacts throughout crystal structures,[1] a lot of work has been addressed to gain control on the preparation of tailored crystal arrangements. The properties of the crystalline material will depend on its individual components and on the manner they arrange and interact in the crystalline state.[2,3] The way and strength of the intermolecular interactions depend on the inorganic or organic nature of the individual components. Inorganic systems can be classified into two categories. In the first one, the extended networks are formed through metal−ligand coordination bonds; in the second one, the building blocks are linked through weaker noncovalent interactions as hydrogen bonding, $\pi-\pi$ stacking, van der Waals forces, etc.[4−6] Metal ions can strongly affect the electron density of

* Authors to whom correspondence should be addressed. E-mail: enrique.garcia-es@uv.es (E.G.-E.); hodacova@uochb.cas.cz (J.H.).
[†] Academy of Sciences of the Czech Republic.
[‡] Instituto de Ciencia Molecular, Universidad de Valencia.
[§] Instituto de Materiales, Universidad de Valencia.
[||] SCSIE, Universidad de Valencia.
[⊥] UAMOA, Universitat Jaume I/CSIC.

(1) (a) Cohen, M. D.; Schmidt, G. M. J.; Sonntag, F. I. *J. Chem. Soc.* **1964**, 2000−2013. (b) Schmidt, G. M. J. *J. Chem. Soc.* **1964**, 2014−2021. (c) Schmidt, G. M. J. *Pure Appl. Chem.* **1971**, *27*, 647−678.
(2) (a) Lehn, J. M. *Supramolecular Chemistry. Concepts and Perspectives*; VCH: Weinheim, 1995. (b) Atwood, J. L.; Barbour, L. J. *Cryst. Growth Des.* **2003**, *3* (1), 3−8.
(3) (a) Desiraju G. R. *Nature* **2001**, *412*, 397−400. (b) Hosseini, M. W. *Acc. Chem. Res.* **2005**, *38* (4), 313−323.

10.1021/ic051099j CCC: $30.25
Published on Web 09/20/2005

Chart 1

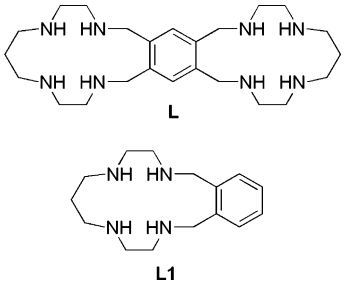

the functional groups present in their neighborhood and thereby the strength of intermolecular interactions. On the other hand, the counterions present in the crystal are rarely innocent with respect to the arrangement of the different components. Anions, apart from charged species, are Lewis bases that tend to accept hydrogen bonds and therefore contribute to the ordering of the crystal lattice.[7]

Here we report on a ditopic cyclophane ligand in which two 1,5,8,12-tetraamine molecules have been attached through methylene spacers to the ortho positions of a benzene ring (see **L** in Chart 1). This compound has a skeleton that reminds a butterfly. The butterfly core would be defined by the benzene ring while the polyamine bridges would be forming the wings. In this paper, we present three new crystal structures; the first one corresponds to the tetraprotonated free macrocycle ($H_4\mathbf{L}^{4+}$) having two tetrachlorozincate(II) counteranions, the second one is of a binuclear Cu^{2+} complex having coordinated chloride anions and perchlorate counteranions, and the third one corresponds to an analogous Zn^{2+} complex that has been crystallized using triflate as counteranion. The analysis of the crystallographic data clearly shows that the relative disposition of the wings of the macrocycle and, in consequence, the overall architecture of the crystals are controlled by the anions present in the moiety, $\pi-\pi$ stacking between the aromatic rings, and hydrogen bonding interactions involving the anions and the water used as the solvent.

In addition, we have studied the protonation behavior and stability constants for the formation of the Cu^{2+} and Zn^{2+} complexes in aqueous solution. Intramolecular hydrogen-bonding formation defines the protonation behavior of the compound. Positive cooperativity is observed in the formation of the Cu^{2+} complexes.

Experimental Section

Materials. All chemicals and solvents were obtained from commercial sources and used without further purification. Compound **L** was synthesized as previously reported[8] and isolated as the hydrochloride salt of formula $\mathbf{L}\cdot 8HCl\cdot 2H_2O$.

Synthesis of the Complexes. $[H_4L](ZnCl_4)_2\cdot 2H_2O$ (1). Colorless crystals of **1** suitable for X-ray analysis were obtained from an aqueous solution at an initial pH of 7 containing equimolar amounts of $Zn(ClO_4)_2$ and $\mathbf{L}\cdot 8HCl\cdot 2H_2O$. Slow evaporation without further control of the pH produced acidification of the moiety inducing formation of uncoordinated $ZnCl_4^{2-}$ species. Yield: 27%. Anal. Calcd for $C_{24}H_{54}O_2N_8Cl_8Zn_2$: C, 31.98; H, 6.04; N, 12.43 (M_r = 901.14). Found: C, 31.90; H, 5.86; N, 12.01.

$[Cu_2LCl_2](ClO_4)_2\cdot 6H_2O$ (2). Blue crystals of **2** were obtained by slow evaporation of an aqueous solution containing equimolar amounts of $Cu(ClO_4)_2$ and $\mathbf{L}\cdot 8HCl\cdot 2H_2O$. Yield: 49%. Anal. Calcd. for $C_{24}H_{58}O_{14}N_8Cl_4Cu_2$: C, 30.29; H, 6.14; N, 11.77 (M_r = 951.7). Found: C, 30.41; H, 6.81; N, 11.59.

CAUTION! Perchlorate salts are potentially explosive and have to be handled with care.

$[Zn_2LCl_2](CF_3SO_3)_2\cdot 0.6H_2O$ (3). Colorless crystals of **3** were grown from an aqueous solution at pH 9 containing $Zn(CF_3SO_3)_2$ and $\mathbf{L}\cdot 8HCl\cdot 2H_2O$ in 2:1 molar ratio. Yield: 56%. Anal. Cald. for $C_{26}H_{47.2}O_{6.6}N_8Cl_2F_6S_2Zn_2$: C, 32.57; H, 4.92; N, 11.69 (M_r = 958.71). Found: C, 32.71; H, 5.10; N, 11.22.

Electromotive Force (emf) Measurements. Potentiometric titrations were carried out in 0.15 mol dm^{-3} $NaClO_4$ at 298.1 ± 0.1 K by using the experimental procedure (buret, potentiometer, cell, stirrer, microcomputer, etc.) that has been fully described elsewhere.[9] The acquisition of the emf data was performed with the computer program PASAT.[10] The reference electrode was a Ag/AgCl electrode in saturated KCl solution. The glass electrode was calibrated as a hydrogen ion concentration probe by titration of well-known amounts of HCl with CO_2-free NaOH solutions and determination of the equivalent point by Gran's method,[11] which gives the standard potential $E^{\circ\prime}$ and the ionic product of water [pK_w = 13.73(1)]. The computer program HYPERQUAD[12] was used to calculate the protonation and stability constants, and the HySS[13] program was used to obtain the distribution diagrams. The titration curves for each system (ca. 150 experimental points corresponding to at least three measurements, pH 2−11, concentration of ligands 1×10^{-3} to 5×10^{-3} mol dm^{-3}) were treated either as a single set or as separated curves without significant variations in the values of the stability constants. Finally, the sets of data were merged together and treated simultaneously to give the final stability constants.

ESI Mass Spectroscopy. ESI-MS spectra were recorded with an Esquire 300 (Bruker) by electrospray positive mode (ES^+).

(4) (a) Roesky, H. W.; Andruh, M. *Coord. Chem. Rev.* **2003**, *236* (1−2), 91−119. (b) Dunitz, J. D.; Gavezzotti, A. *Angew. Chem. Int. Ed.* **2005**, *44* (12), 1766−1787.

(5) (a) Epstein, L. M.; Shubina, E. S. *Coord. Chem. Rev.* **2002**, *231* (1−2), 165−181. (b) Steiner, T. *Angew. Chem. Int. Ed.* **2002**, *41* (1), 48−76. (c) Desiraju, G. R. *Acc. Chem. Res.* **2002**, *35* (7), 565−573. (d) Lutz, H. D. *J. Mol. Struct.* **2003**, *646* (1−3), 227−236. (e) Jeffrey, G. A. *Crystallogr. Rev.* **2003**, *9* (2−3), 135−176. (f) Desiraju, G. R. *Chem. Commun.* **2005**, 2995−3001.

(6) (a) Claessens, C. G.; Stoddart, J. F. *J. Phys. Org. Chem.* **1997**, *10* (5), 254−272. (b) Desiraju, G. R.; Steiner, T. *The Weak Hydrogen Bond*; Oxford University Press: Oxford, 1999. (c) Hunter, A.; Lawson, K. R.; Perkins, J.; Urch, C. J. *Perkin Trans. 2* **2001**, *5*, 651−669. (d) Garau, C.; Frontera, A.; Quinonero, D.; Ballester, P.; Costa, A.; Deya, P. M. *Chem. Phys. Lett.* **2004**, *399* (1−3), 220−225.

(7) (a) Bianchi, A., Bowman-James, K., García-España, E., Eds. *Supramolecular Chemistry of Anions*; Wiley-VCH: New York, 1997. (b) Steed, J. W.; Atwood J. L. *Supramolecular Chemistry*; John Wiley & Sons: London, 2000; Chapter 4. (c) Beer, P. D.; Gale, P. A. *Angew. Chem. Int. Ed.* **2001**, *40* (3), 486-516. (d) Beer, P. D.; Hayes, E. J. *Coord. Chem. Rev.* **2003**, *240* (1−2), 167−189.

(8) Chadim M.; Budesinsky M.; Hodacova, J.; Zavada, J. *Collect. Czech. Chem. Commun.* **2000**, *65*, 99−105.

(9) García-España, E.; Ballester, M. J.; Lloret, F.; Moratal, J.-M.; Faus, J.; Bianchi, A. *J. Chem. Soc., Dalton Trans.* **1988**, *2*, 101−104.

(10) Fontanelli, M.; Micheloni, M. *Proceedings of the 1st Spanish-Italian Congress on Thermodynamics of Metal Complexes*, Peñíscola, Castellón (Spain), June 3−6, 1990.

(11) (a) Gran, G. *Analyst* (*London*) **1952**, *77*, 661−671. (b) Rossoti, F. J. C.; Rossoti, H. *J. Chem. Educ.* **1965**, *42*, 375−378.

(12) Gans, P.; Sabatini, A.; Vacca, A. *Talanta* **1996**, *43*, 1739−1753.

(13) Alderighi, L.; Gans, P.; Ienco, A.; Peters, D:, Sabatini, A.; Vacca, A. *Coord. Chem. Rev.* **1999**, *184*, 311.

Table 1. Crystallographic Data for **1**−**3**

	1	**2**	**3**
chemical formula	$C_{24}H_{54}O_2N_8Cl_8Zn_2$	$C_{24}H_{58}O_{14}N_8Cl_4Cu_2$	$C_{26}H_{51.2}O_{6.6}N_8Cl_2F_6S_2Zn_2$
fw (amu)	901.14	951.70	958.71
cryst syst	Triclinic	orthorombic	triclinic
space group	$P\bar{1}$	*F*2*dd*	$P\bar{1}$
T (K)	293(2)	293(2)	293(2)
λ(Mo Kα) (Å)	0.7107300	0.7107300	0.7107300
a (Å)	9.1890(2)	9.9380(2)	8.472(5)
b (Å)	14.0120(3)	30.2470(6)	9.310(5)
c (Å)	15.3180(3)	53.143(1)	13.745(5)
α (deg)	89.2320(7)	90	84.262(5)
β (deg)	82.0740(6)	90	77.490(5)
γ (deg)	83.017(1)	90	73.557(5)
V (Å^3)	1938.95(7)	15974.5(6)	1014.2(9)
Z	2.00	18.00	2.00
d_{calcd} (mg m^{-3})	0.7614	1.5780	1.5720
abs coeff (mm^{-1})	0.911	1.550	1.494
F(000)	453.9	7848.0	495.0
refln collected	12713	8185	6373
unique reflns	8775	8185	4164
data/restrain/parameters	8775/0/495	8185/1/485	4164 /1/336
GOF	0.903	0.777	0.972
R_1[a]	0.0392	0.0572	0.0849
wR_2[b]	0.1127	0.1290	0.2166
largest diff. peak and hole (e·Å^{-3})	0.535 and −0.406	0.716 and −0.346	0.971 and −0.787

[a] $R_1 = \Sigma||F_o| - |F_c||/\Sigma|F_o|$. [b] $wR_2 = \Sigma w(F_o^2 - F_c^2)^2/w(F_o^2)^2$; for **1** and **2**, $w = 1/[\sigma^2(F_o^2) + (0.1000P)^2 + 0{,}0000P]$ and $P = (F_o^2 + 2F_c^2)/3$. For **3**, $w = 1/[\sigma^2(F_o^2) + (0.1254P)^2 + 1.9563P]$ and $P = (F_o^2 + 2F_c^2)/3$.

X-ray Structure Study. Analysis on single crystals of the complexes was performed at 293 K on a Nonius Kappa-CCD single-crystal diffractometer, using Mo Kα radiation ($\lambda = 0.7107300$ Å). Data collection strategy was calculated with the program Collect.[14] Data reduction and cell refinement were performed with the programs HKL, Denzo, and Scalepack.[15] The unit cell dimensions were measured from the angular settings of 6381 reflections between $\theta = 0.998°$ and 27.49° for **1**, 4423 reflections between $\theta = 2.910°$ and 27.49° for **2**, and 5606 reflections between $\theta = 0.998°$ and 27.49° for **3**.

The crystal structures were solved by the Patterson method, using the program DIRDIF96.[16] Anisotropic least-squares refinement was carried out with SHELXL97.[17] All non-hydrogen atoms were anisotropically refined. Hydrogen atoms were located in a difference Fourier map, and the rest were located geometrically. Lorenz and polarization corrections were applied, and the data were reduced to $|F_o|$ values.

Geometrical calculations were made with PARST.[18] The crystallographic plots were made with the ORTEP[19] and/or MERCURY programs.[20]

(14) *COLLECT*, Nonius BV, 1997−2000.

(15) DENZO−SCALEPACK. Otwinowski, Z.; Minor, W. Processing of X-ray diffraction data collected in oscillation mode. In *Methods in Enzymology, Volume 276*: *Macromolecular Crystallography, Part A*; Carter, C. W., Jr., Sweet, R. M., Eds.; Academic Press: New York, 1997; pp 307−326,

(16) DIRDIF96 program system. Beurskens, P. T.; Beurskens, G.; Bosman, W. P.; de Gelder, R.; Garcia-Granda, S.; Gould, R. O.; Israel, R.; Smits, J. M. M. The DIRDIF96 Program System. Technical Report of the Crystallography Laboratory, University of Nijmegen, The Netherlands, 1996.

(17) SHELX97. Sheldrick, G. M. *SHELX97. Programs for Crystal Structure Analysis* (Release 97-2); University of Göttingen: Göttingen, Germany, 1997.

(18) PARST. (a) Nardelli, M. *Comput. Chem*. **1983**, *7*, 95−97. (b) Nardelli, M. *J. Appl. Crystallogr*. **1995**, *28*, 659.

(19) ORTEP3 for Windows. Farrugia, L. J. *J. Appl. Crystalogr*. **1997**, *30* (5, Pt. 1), 565.

(20) MERCURY 1.3 for Windows Me/2000/XP. (a) Bruno, I. J.; Cole, J. C.; Edgington, P. R.; Kessler, M. K.; Macrae, C. F.; McCabe, J.; Pearson, J.; Taylor, R. *Acta Crystallogr*. **2002**, *B58*, 389−397. (b) Taylor, R.; Macrae, C. F. *Acta Crystallogr*. **2001**, *B57*, 815−827.

Table 2. Equilibrium Constants for the Systems H^+-**L**, Cu^{2+}-**L**, and Zn^{2+}-**L** Determined in 0.15 mol dm^{-3} $NaClO_4$ at 298.1 ± 0.1 K

	system		
reaction[a]	H^+-**L**	Cu^{2+} -**L**	Zn^{2+}-**L**
$H + L \leftrightarrows HL$			
$2H + L \leftrightarrows H_2L$	21.85(4)[b]		
$H_2L + H \leftrightarrows H_3L$	9.80(3)		
$H_3L + H \leftrightarrows H_4L$	9.14(4)		
$M + L \leftrightarrows ML$			14.43(5)
$M + L + 2H \leftrightarrows MH_2L$		37.87(7)	-
$2M + L \leftrightarrows M_2L$		34.95(4)	26.95(5)
$ML + M \leftrightarrows M_2L$			12.52(5)
$M_2L + H \leftrightarrows M_2HL$		4.50(4)	5.66(3)
$M_2L + H_2O \leftrightarrows M_2L(OH) + H$			−10.01(3)

[a] Charges omitted for clarity. [b] Values in parentheses are standard deviations in the last significant figure.

Table 3. Selected Hydrogen-Bond Distances and Angles for **1**

distances, Å		angles, deg	
N(1)−N(4)	2.860(4)	N(4)−H(4D)−N(1)	154(3)
N(5)−N(8)	2.847(4)	N(5)−H(5D)−N(8)	149(4)
N(6)−N(7)	2.740(4)	N(7)−H(7D)−N(6)	154(4)
N(4)−Cl(7)	3.175(3)	N(4)−H(5)−Cl(7)	145(3)
O(1)−O(2)	2.998(5)	O(2)−H(204)−O(1)	171(4)
O(1)−N(5)	2.856(5)	N(5)−H(8)−O(1)	175(4)
O(1)−Cl(1)	3.167(4)	O(1)−H(204)−Cl(1)	141(6)
O(2)−N(2)	2.889(5)	O(2)−H(2)−N(2)	142(4)

The crystallographic data are summarized in Table 1. Selected bond lengths and bond angles for the complexes are listed in Tables 3−6.

Results and Discussion

Protonation and Metal Complex Formation in Solution. Table 2 gathers the stepwise basicity constants of **L** and the constants for the formation of Cu^{2+} and Zn^{2+} complexes of **L** determined in 0.15 mol dm^{-3} $NaClO_4$ at 298.1 K.

L has, in the pH range 2.0−11.0, four measurable constants from a total of eight possible ones. The last four

Table 4. Selected Distances and Angles for Complex **2**

	Distances, Å		
Cu(1)−Cl(2)	2.711(2)	Cu(2)−Cl(3)	2.678(2)
Cu(1)−N(1)	2.073(7)	Cu(2)−N(5)	2.041(7)
Cu(1)−N(2)	2.029(7)	Cu(2)−N(6)	2.027(8)
Cu(1)−N(3)	2.048(7)	Cu(2)−N(7)	2.058(8)
Cu(1)−N(4)	2.044(7)	Cu(2)−N(8)	2.070(8)
	Angles, deg		
Cl(2)−Cu(1)−N(1)	90.5(2)	N(2)−Cu(1)−N(3)	90.6(2)
Cl(2)−Cu(1)−N(2)	92.7(2)	N(3)−Cu(1)−N(4)	84.1(3)
Cl(2)−Cu(1)−N(3)	95.9(3)	N(5)−Cu(2)−N(6)	84.0(3)
Cl(2)−Cu(1)−N(4)	91.6(2)	N(5)−Cu(2)−N(8)	100.4(2)
N(1)−Cu(1)−N(2)	84.2(3)	N(6)−Cu(2)−N(7)	91.4(3)
N(1)−Cu(1)−N(4)	100.6(2)	N(7)−Cu(2)−N(8)	83.8(3)

Table 5. Selected Hydrogen Bond Distances for Complex **2**

	Distances, Å		
Cl(2)−O(200)	3.137(8)	O(300)−Cl(3)	3.13(1)
O(200)−O(100)	2.89(1)	O(600)−O(500)	2.68(2)
O(100)−O(600)	2.71(1)	O(500)−O(21)	2.73(2)
O(600)−O(400)	2.59(2)	O(500)−O(24)	2.92(2)
O(400)−Cl(2)	3.13(1)	O(200)−O(300)	2.80(1)
O(300)−O(400)	2.62(1)	O(100)−Cl(3)	3.07(1)

Table 6. Selected Distances and Angles for Complex **3**

	Distances, Å		
Zn(1)−N(1)	2.127(7)	Zn(1)−N(4)	2.153(8)
Zn(1)−N(2)	2.151(8)	Zn(1)−Cl(1)	2.128(7)
Zn(1)−N(3)	2.14(1)	Zn(1)−Cl(1)	2.504(7)
	Angles, deg		
N(1)−Zn(1)−N(2)	82.4(3)	N(3)−Zn(1)−N(2)	84.9(4)
N(1)−Zn(1)−N(3)	157.4(4)	N(3)−Zn(1)−N(4)	82.4(3)
N(1)−Zn(1)−N(4)	102.7(3)	N(3)−Zn(1)−Cl(1)	92.3(5)
N(1)−Zn(1)−Cl(1)	108.5(3)	N(3)−Zn(1)−Cl(1)	108.0 (5)
N(1)−Zn(1)−Cl(1)	92.9(3)	Cl(1)−Zn(1)−N(2)	101.2(3)
N(2)−Zn(1)−N(4)	157.1(4)	Cl(1)−Zn(1)−N(4)	98.3(3)

protonation steps are too low to be detected by means of potentiometric measurements whereas the first two protonation constants are high and very close between them; thus, they appear together with an overall value of 21.85(4) logarithmic units. These basicity constants can be interpreted taking into account the formation of intramolecular hydrogen bonds within each one the macrocyclic wings. Such a behavior was also observed for 2,5,8,11-tetraaza[12]*o*-cyclophane (**L1**) (see Chart 1),[21] although in that case neither the basicity of the last steps nor the acidity of the first ones was so high as in the double macrocycle. Among others, statistical factors would favor the higher basicity of **L** with respect to **L1**. On the other hand, the breaking of the hydrogen bond framework between alternated amino and ammonium groups is very energetically demanding and yields constants too low for being measured. The macrocycle cyclam is another clear example of a similar behavior.[22]

The most significant aspect of the constants collected in Table 2 for the system Cu^{2+}-**L** is the existence of a positive cooperative binding.[23] Distribution diagrams calculated for a Cu^{2+}:**L** 1:1 mole ratio show the predominant formation of 2:1 species above pH 7. Therefore, the entry of the first metal

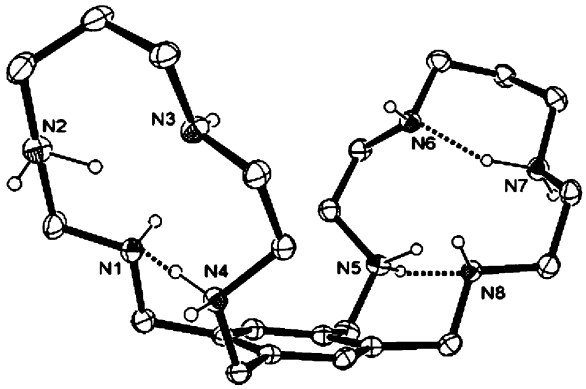

Figure 1. ORTEP drawing of $[H_4L]^{4+}$ cation-forming complex **1**. Thermal ellipsoids are drawn at the 25% of probability level. Only the hydrogen atoms involved in intramolecular hydrogen bonding are shown.

organizes the macrocycle favoring the second metal uptake. In view of the crystal structures discussed below, the anions present in the medium might play a significant role in such a behavior. Indeed, MS-ESI spectra of aqueous solutions containing Cu^{2+} and **L** in mole ratio 2:1 show a peak at *m*/*z* 743.1 as a base peak that can be ascribed to the $[Cu_2\mathbf{L}Cl_2(ClO_4)]^+$. These unit fragments loosing successively the two chloride anions (*m*/*z* 705.1 and 669.0) and retaining the perchlorate anion. Another peak in the MS-ESI spectra appears at *m*/*z* 807.0 that can be attributed to a $[Cu_2\mathbf{L}Cl(ClO_4)_2]^+$ unit (Supporting Information) Further studies would be performed in order to address this correspondence between the solution and solid-state structures.

In the case of the Zn^{2+} complexes, however, the second stepwise constant ($\log K_2 = 12.52$) is lower than the first one ($\log K_1 = 14.43$) indicating the absence of a clear positive cooperativity (Table 2). The crystal structure of the complex $[Zn_2\mathbf{L}Cl_2](CF_3SO_3)_2\cdot 0.6H_2O$ (**3**) (vide infra) might help explaining this behavior due to the extended chair conformation that the macrocycle adopts upon formation of the binuclear complex.

Crystal Structure of $[H_4L](ZnCl_4)_2\cdot 2H_2O$ (1). Evaporation of solutions at ca. pH 7 containing $Zn(ClO_4)_2\cdot 6H_2O$ and **L**·8HCl·$2H_2O$ in 2:1 M:**L** mole ratio yielded crystals of $[H_4\mathbf{L}](ZnCl_4)_2\cdot 2H_2O$ suitable for X-ray analysis. As can be deduced from the speciation studies, pH 7 is a borderline pH where the percentage of complexed Zn^{2+} is still low. Under these conditions, evaporation produced crystals of a compound in which a tetraprotonated macrocycle behaves as countercation of complex units in which four chloride anions are coordinated to the Zn^{2+} with tetrahedral disposition ($ZnCl_4^{2-}$ units). The butterfly-like macrocyclic units adopt a boat-shaped conformation in which both "wings" are oriented toward the same side of the macrocyclic cavity (see Figure 1). The opening angle between the wings of the macrocycles defined by the mean planes going through nitrogen atoms N(1)−N(2)−N(3)−N(4) (wing 1) and N(5)−N(6)−N(7)−N(8) (wing 2) is 55.6(1)°. The angles formed

(21) Chadim, M.; Díaz, P.; Garcia-España, E.; Hodacova, J.; Junk, P. C.; Latorre, J.; Llinares, J. M.; Soriano, C.; Zavada, J. *New J. Chem.* **2003**, *27* (7), 1132−1139.

(22) Martell, A. E.; Smith, R. M.; Moteikaitis, R. J. *NIST Critical Stability Constants of Metal Complexes Database NIST Standard*, Reference Database, Version 4, 1997.

(23) (a) Onufriev, A.; Ullmann, G. M., *J. Phys. Chem. B* **2004**, *108*, 1157−1169. (b) Williams, D. H.; Stephens, E.; O'Brien, D. P.; Zhou, M. *Angew. Chem. Int. Ed.* **2004**, *43*, 6596−6616. (c) Leigh, D. A. *Chem. Biol.* **2003**, *10* (12), 1143−1144. (d) Robertson, A.; Shinkai, S. *Coord. Chem. Rev.* **2000**, *205*, 157−199. (d) Di Cera, E. *Chem. Rev.* **1998**, *98* (4), 1563−1591.

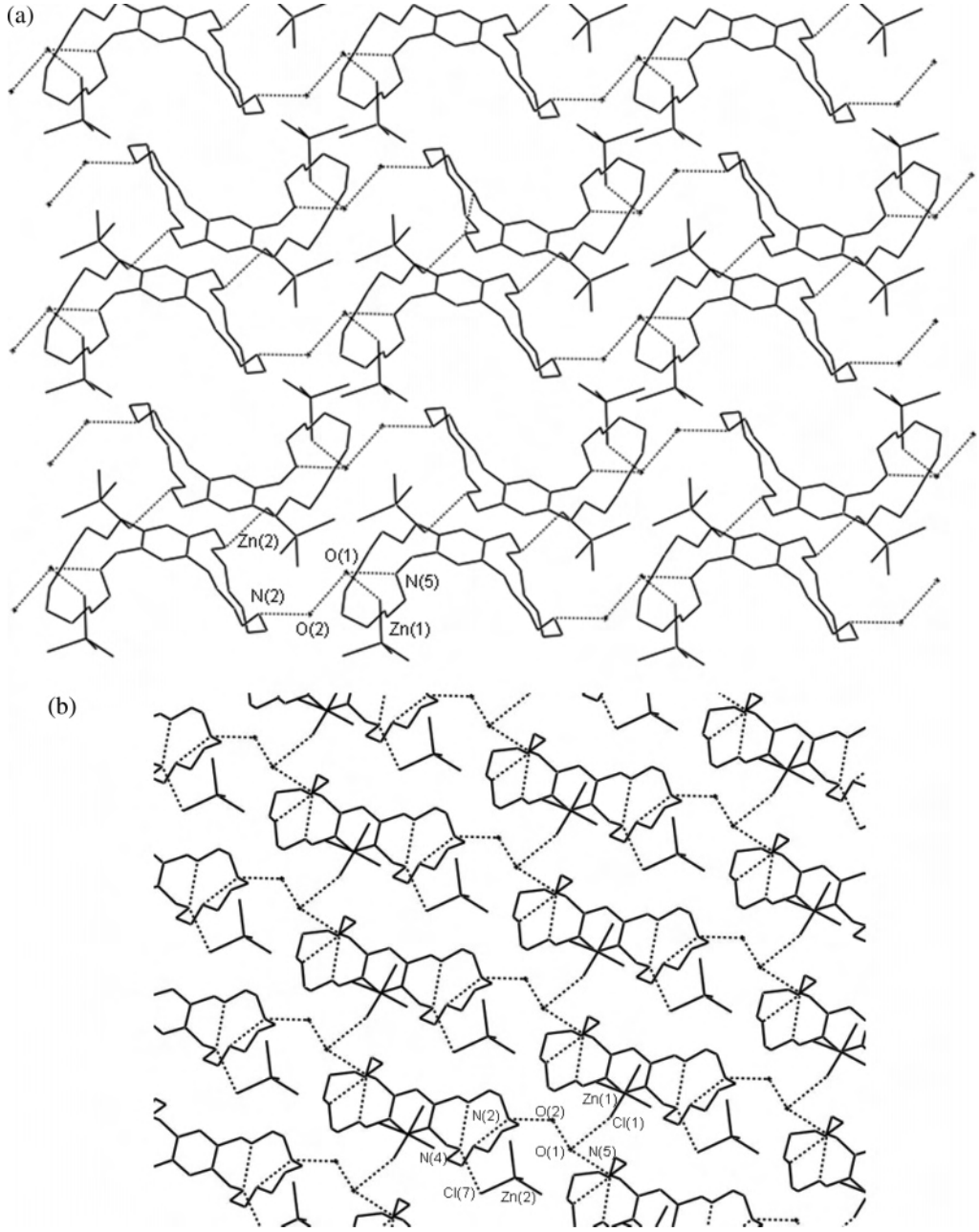

Figure 2. (a) View of the crystal packing of **1** showing the $\pi-\pi$ stacking interactions and the two different types of $ZnCl_4^{2-}$ counteranions labeled as Zn1 and Zn2. (b) View of the crystal packing of **1** showing labeling of atoms involved in main intermolecular hydrogen bonds. In this view it is shown as one type of $ZnCl_4^{2-}$ anions is partially embedded within the clefts of the macrocycles in the contiguous row. Hydrogen atoms omitted for clarity.

by wing 1 and wing 2 with the plane of the aromatic ring which define the opening of each one of the wings are of 60.7(1)° and 65.78(9)°, respectively.

The reason for this boat conformation is at least 3-fold. First, each diprotonated tetraamine bridge displays an intramolecular hydrogen bond network involving the alternated protonated and nonprotonated amino groups N(6)···N(7), N(5)···N(8) in wing 2 and N(1)···N(4) in wing 1 (Table 3), which might be stabilizing the boat conformation; protonated N(2) in wing 1 forms an additional hydrogen bond with a water molecule. Second, the macrocycles are π-stacked in couples, and a boat-shaped conformation favors this organization (Figure 2a). Third, and most importantly, one of the $ZnCl_4^{2-}$ anions is almost encapsulated within the cleft of the macrocycle counterbalancing partly its positive charge (Figure 2b and Figure S4).

The packing of the crystal can be basically defined as a double-chain 2-D row of boat-shaped macrocycles. The macrocycles constituting a chain are interconnected by hydrogen bonds between one protonated amino group of each macrocycle and a relay of two water molecules (N(2)−O(2), O(2)−O(1), and O(1)−N(5)) (see Figure 2 and Table 3). The two chains are associated between them by π-stacking. The distance between the planes of the aromatic rings is 3.49 Å, which are shifted one with respect to the other by 3.16 Å.

The double chain motifs are interconnected through hydrogen bonding of the pseudo-encapsulated tetrachlorozincate and the oxygen atom of a water molecule (O(1)−Cl-

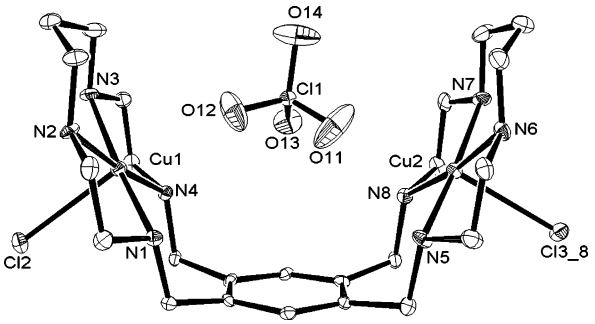

Figure 3. ORTEP drawing of the $[Cu_2\mathbf{L}Cl_2]^{3+}$ cation including the encapsulated ClO_4^- anion. Thermal ellipsoids are drawn at the 10% probability level. Hydrogens omitted for clarity.

(1)). The other $ZnCl_4^{2-}$ anion is hydrogen bonded to N(4) of the macrocycles (N(4)−Cl(7)) (Table 3) contributing to maintain the closure of the wings and is occupying an empty space in the layer.

Crystal Structure of $[Cu_2LCl_2](ClO_4)_2\cdot 6H_2O$ (2). The crystal structure consists of $[Cu_2\mathbf{L}Cl_2]^{2+}$ cations, two crystallographicaly different perchlorate anions and water molecules. The coordination geometry around each Cu^{2+} ion can be defined as a strongly axially distorted square pyramid. In both coordination centers the equatorial plane is formed by four nitrogen atoms of the macrocyclic ring while the axial position is occupied by a chloride atom that points outside the cleft formed by the two coordination planes and the plane of the aromatic spacer (Figure 3). The metal atoms are coplanar with the mean plane passing through the four nitrogen atoms in each coordination site (Cu(1) and Cu(2) elevations with respect to the planes are 0.091(1) and 0.098(2) Å, respectively). The average Cu−N distance is 2.06 Å in both coordination sites, and the Cu−Cl distance differs slightly from one site to the other (Table 4). The angles in the coordination sphere are almost normal.

It is interesting to remark that the wings of the butterfly molecule are oriented toward the same side of the aromatic ring giving again a boat conformation with a separation between the metal ions of 7.100 (1) Å. However, the most favorable conformation from an electrostatic point of view should, in principle, be the opposite one, in which the two wings extend toward different sides of the aromatic ring (chair conformation). The main reason for the boat conformation observed resides in that one of the two perchlorate anions is included within the cleft interacting axially at large distance with Cu(1) (Cu(1)−O(12) = 2.83 Å) and forming a hydrogen bond with N(5). Therefore, this counteranion balances the electrostatic repulsion between the metal ions favoring the closure of the wings. The angle between both coordination planes has been calculated to be 70.0(2)° and is larger than the one observed in the previously discussed structure. However, the opening of both wings with respect to the aromatic ring is slightly different; the angle between the wing defined by the coordination plane around Cu(1) and the aromatic ring is 53.8(2)° while that defined by the coordination plane including Cu(2) is 56.4(2)°.

The most relevant aspect of this crystal structure is its three-dimensional arrangement (Figure 4). The different boat-shaped molecules are puckered together by π-stacking interactions and by an interesting hydrogen bond framework. The mean distance between the planes defined by the benzene rings is 3.36 Å, which are shifted one with respect to the other by 1.63 Å.

The hydrogen-bond network involves the coordinated chloride anions, the lattice water molecules, and the oxygen atoms of the perchlorate counteranions located outside the macrocyclic cavity. This network might be basically defined as chains of pentamer units interconnected by rhomboid motifs (Figure 5).

Each pentamer motif is defined by the metal-coordinated chloride atom labeled Cl(2) and the oxygen atoms of four independent water molecules (O(400), O(600), O(100) and O(200)) (see Figure 5a). The vertexes of the rhomboids,

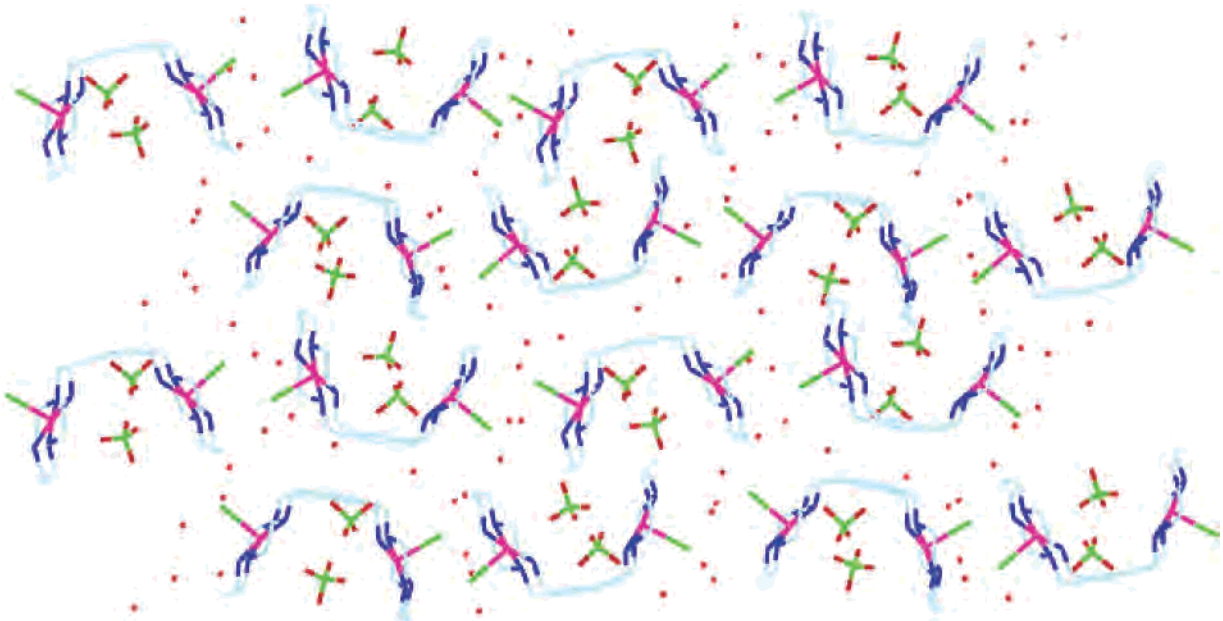

Figure 4. Crystal packing of **2** along the *a* axis. Hydrogen atoms omitted for clarity. Red points represent water molecules placed inside the channels defined by the packing.

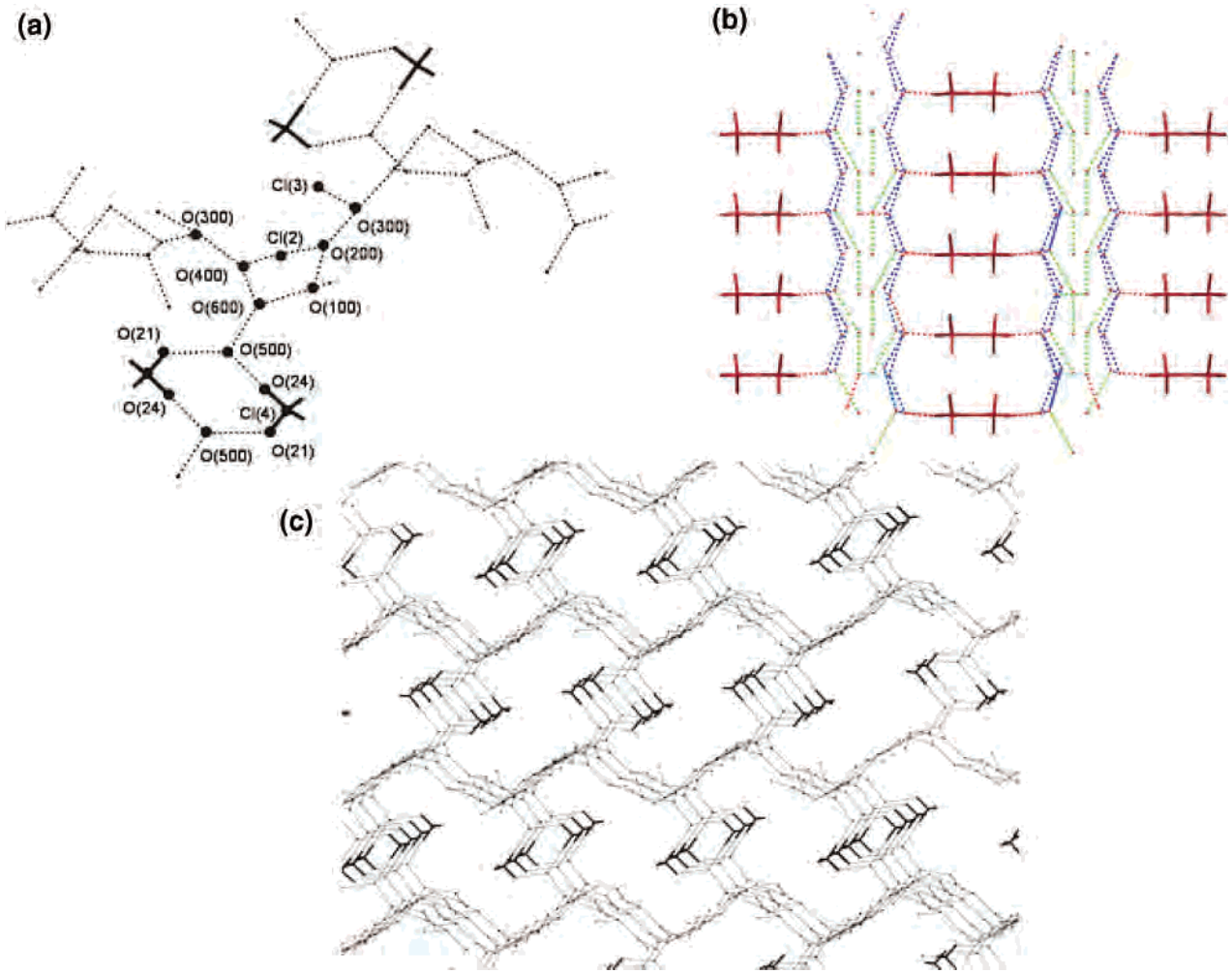

Figure 5. Details of the hydrogen-bond network characteristic of **2**. (a) Labeling of the atoms involved in the pentamer and rhomboid motifs. (b) View along the *b* axis where it is possible to distinguish in detail the two pentamer chains (vertical blue) linked by the rhomboid motifs (horizontal red colored). (c) View of the network along the *a* axis.

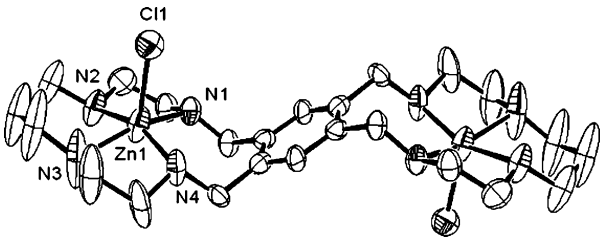

Figure 6. ORTEP drawing of the $[Zn_2\mathbf{L}Cl_2]^{2+}$ cation. Thermal ellipsoids at the 50% probability level. Hydrogens omitted for clarity.

which have internal 2-fold symmetry, are built by the chloride atoms Cl(4) of two equivalent perchlorate anions and two oxygens O(500) of two equivalent water molecules. The pentamers are interconnected through O(300) of a water molecule forming a sort of zig-zag chain. The rhomboids units link the pentamer-chains through hydrogen-bonds involving O(600) and O(500) (Figure 5a). All this arrangement sets up a 3-D net of interconnected bubbles in which the macrocycles are embedded (Figure 4). Thus, every chloride atom of a macrocycle is associated with the nonequivalent chloride of its related stacked counterpart through a hydrogen bonding involving O(400) of a pentagon and O(300), which bridges between pentagons. On the other hand, every oppositely oriented macrocycle of different couples are connected by the hydrogen bonding path [Cl(2)···O(200)···O(300)···Cl(3)] and by a long hydrogen bond of Cl(2) with the amino group N(7) of the opposite unit.

Crystal Structure of $[Zn_2\mathbf{L}Cl_2](CF_3SO_3)_2\cdot 0.6H_2O$ (3). Colorless crystals suitable for X-ray diffraction were obtained after slow evaporation of aqueous solutions containing equimolar amounts of $Zn(CF_3SO_3)_2$ and **L**·8HCl at pH = 9. The pH was set high enough to avoid any dissociation of the metal ion along the crystallization process the way it happened when **1** was obtained.

The crystal structure consists of $[Zn_2\mathbf{L}Cl_2]^{2+}$ complex cations, $CF_3SO_3^-$ counteranions, and lattice water molecules. In each equivalent wing, the Zn^{2+} atoms are coordinated in a square pyramidal fashion with the four nitrogens occupying the equatorial plane and one chloride anion in the axial position (Figure 6). The average Zn−N distance is 2.15 Å. The structure has a positional disorder with the coordinated chloride atom located in two different positions with Zn−Cl distances of 2.14 or 2.50 Å.

Interestingly, in contrast with the other two reported structures, in this one the macrocycle adopts a chair conformation with the butterfly wings extended toward

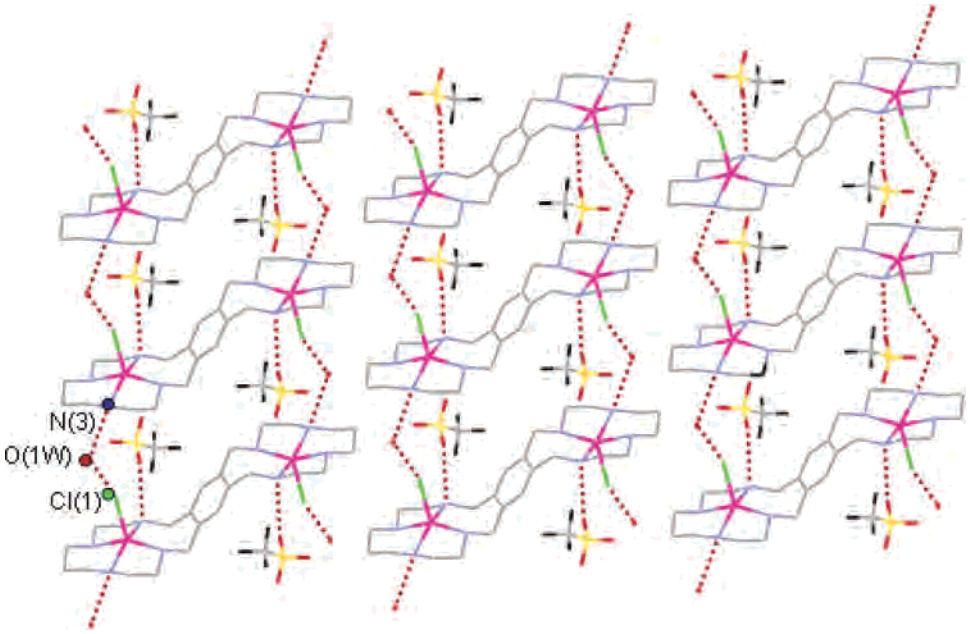

Figure 7. View of the packing of **3**. Hydrogen atoms and disordered chloride atom omitted for clarity.

distinct sides of the benzene core. As commented before, this chair conformation would be, in the absence of other factors, the most favorable one from an electrostatic point of view, since in this way the coordinated metal ions lie 9.10 Å apart. In this case, the size and geometry of the triflate counteranions are not appropriated to allow its location between the coordinated wings as occurred with the perchlorate or tetrachlorozincate anions of the previously discussed structures. In consequence, the absence of a negative species minimizing the repulsion resulting from the approach of the two coordinated wings induces the macrocyclic complex to adopt a chair conformation instead of the boat one. Moreover, it has to be pointed out that there is no π-stacking between the units (Figure 7).

The chair-shaped macrocycles bridge each other in rows by two hydrogen bonds implicating the chloride anions Cl(1) coordinated at a larger distance, the oxygen O(1W) of a water molecule, and the N(3) of a different macrocycle. The 3-D packing would be the result of the alignment of all these straight rows (Figure 7). This time the structural role played by the anions is not significant, thus they are just linked by hydrogen bonding between their O(12) and N(1) of each wing of the macrocycles.

Conclusions

The analysis of the crystallographic data of the three crystal structures reported clearly shows that the overall architecture of the crystals are controlled by the anions present in the moiety, $\pi-\pi$-stacking between the aromatic rings, and hydrogen bonding interactions involving the anions and the water used as the solvent. Tetrahedral anions such as the perchlorate ones can be totally or partially encapsulated in the macrocyclic cleft neutralizing the excess of positive charge favoring boat conformation and stacking between units. On the contrary, larger triflate anions, which have less charge density and cannot be included in the cavity, favor a chair disposition with maximum separation between positive charges and disrupts stacking associations. Hydrogen bonding networks involving water molecules, the counteranions, and metal coordinated halide anions contribute to dictate the growing pattern. A very particular extended 3-D hydrogen network of pentamer and rhomboid units has been observed in the case of the Cu^{2+} complex (**2**). In such structure the water molecules are placed in channels located between the macrocyclic complex units. The understanding derived from the structural and connective features included within these structures may help the construction of tailored inorganic−organic frameworks.

Acknowledgment. Financial support from Grupos S03/196 and DGICYT Project BQU2003-09215-CO3-01 and BQU2003-09215-CO3-02 (Spain) is gratefully acknowledged. P.D. thanks former MCYT for her Ph.D. grant and current Ministerio de Educación y Ciencia for her "Juan de la Cierva" Research Contract. J.M.L. thanks MCYT for his "Ramón y Cajal" contract. We also thank the Academy of Sciences (AVOZ40550506) and Grant Agency (203/98/0726) of the Czech Republic for financial support.

Supporting Information Available: CIF format for the three crystal structures; Figures S1−S3, ESI-MS spectra without and with fragmentation of aqueous solution s containing Cu^{2+} and **L** in molar ratio 2:1 at pH = 8; Figure S4, view of the packing of $[H_4\mathbf{L}](ZnCl_4)_2 \cdot 2H_2O$ **(1)** showing the two types of $ZnCl_4^{2-}$ anions; Figure S5, (a) ^{1}H NMR spectrum of **L** at pD 7.4 in D_2O; (b) ^{1}H NMR spectrum of **L**:Zn^{2+} (1:2) at pD 7.4 in D_2O. This material is available free of charge via the Internet at http://pubs.acs.org.

IC051099J